



Ricerca di Sistema elettrico

# ALFRED Fuel Element Hexagonal Wrapper Conceptual Design

A. Palumbo, G. Grasso, F. Lodi

ALFRED Fuel Element Hexagonal Wrapper Conceptual Design

A. Palumbo (Università di Bologna), G. Grasso (ENEA), F. Lodi (Università di Palermo)

Settembre 2018

Report Ricerca di Sistema Elettrico

Accordo di Programma Ministero dello Sviluppo Economico - ENEA

Piano Annuale di Realizzazione 2017

Area: Generazione di Energia Elettrica con Basse Emissioni di Carbonio

Progetto: Sviluppo competenze scientifiche nel campo della sicurezza nucleare e collaborazione ai programmi internazionali per il nucleare di IV Generazione.

Linea: Collaborazione ai programmi internazionali per il nucleare di IV Generazione

Obiettivo: Progettazione di sistema e analisi di sicurezza

Responsabile del Progetto: Mariano Tarantino, ENEA

**Titolo**
**ALFRED Fuel Element Hexagonal Wrapper Conceptual Design**
**Descrittori**

**Tipologia del documento:** Rapporto Tecnico  
**Collocazione contrattuale:** Accordo di programma ENEA-MSE su sicurezza nucleare e reattori di IV generazione  
**Argomenti trattati:** Termomeccanica, Tecnologia dei reattori nucleari, Generation IV reactors

**Sommario**

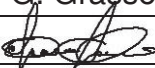
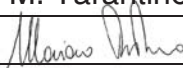
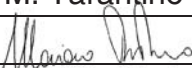
The aim of the work presented in this report is to understand and analyze the issue of differential deformation of the wrapper of a fuel assembly, so as to predict its bending anticipated at end of life.

Despite the simplifications adopted for this ab-initio investigation (i.e., free deformations of the assemblies), the results provide relevant information to orient the design of the ALFRED core restraint system. At the same time, the tool developed to implement the used methodology sets the basis for the development of a more complex analysis tool able to assess the collective behavior of the core under the hypothesis of the mutual interaction between the assemblies.

**Note**

Authors: A. Palumbo<sup>1</sup>, G. Grasso<sup>2</sup>, F. Lodi<sup>3</sup>  
<sup>1</sup>Università di Bologna  
<sup>2</sup>ENEA  
<sup>3</sup>Università di Palermo

**Copia n.**
**In carico a:**

2			NOME			
			FIRMA			
1			NOME			
			FIRMA			
0	EMISSIONE	26/11/2018	NOME	G. Grasso	M. Tarantino	M. Tarantino
			FIRMA			
REV.	DESCRIZIONE	DATA		REDAZIONE	CONVALIDA	APPROVAZIONE

 <b>Ricerca Sistema Elettrico</b>	<b>Sigla di identificazione</b>	<b>Rev.</b>	<b>Distrib.</b>	<b>Pag.</b>	<b>di</b>
	ADPFISS – LP2 – 156	0	L	2	11

## Table of Contents

1. Introduction .....	3
2. Phenomenological description .....	3
3. Model description .....	4
4. Methodology and assumptions .....	6
5. Results .....	9
5.1. Single fuel assembly .....	9
5.2. Row of adjacent fuel assemblies .....	10
6. Conclusions .....	11
References .....	11

## 1. Introduction

Differently from thermal-spectrum reactors, where the limited fuel enrichment and the necessary presence of a moderator in due volume fraction imply significant reactivity feedback effects (respectively: the fuel Doppler effect and the coolant/moderator density effect), fast-spectrum reactors are characterized by many more feedback effects, each much lower in absolute terms hence altogether concurring to determining the inherent response of the system in case of unprotected accidental events.

Among the most important reactivity effects of a fast-spectrum reactor, the modifications of the core geometry are responsible for the insertion of remarkable reactivities (either positive or negative following a core compaction or expansion, respectively).

Accordingly, a core system able to prevent compactions leading to non-manageable positive reactivity insertions, while free to expand upon temperature increases so as to provide the system with an inherent anti-reactivity concurring to the management of events involving the loss-of-flow and/or loss-of-heat-sink, is one of the main objectives of the core design.

Also, since the assemblies are tightly packed in the core lattice, any deformation may easily result in interactions among neighboring elements. In turn, the forces associated to these interactions may be responsible for criticalities in the insertion/withdrawal of the assemblies in/from the core, possibly impairing the capabilities of the refueling machine to handle the loads resulting from the lack of clearance in the core lattice. As in the previous case, a core system able to guarantee the residual interaction forces do not exceed the limits that can be handled by the refueling machine is another main objective of the core design.

These capabilities are strongly related to the design of the core restraint system, which is called to provide at the same time stiffness and freedom to the lattice of sub-assemblies comprising the core.

The study presented in this report is meant at providing an ab-initio insight into the phenomenon of sub-assemblies deformation, and preliminary results on the extent of such deformation on Fuel Assemblies (FAs), as the sub-assemblies most subject to the causes resulting in deformation.

## 2. Phenomenological description

Due to the buckling, the neutron flux and power profiles are not uniform throughout the core. Each assembly is therefore subject to two main effects:

- a temperature gradient (due to the non-uniform power profile);
- an irradiation dose gradient (due to the non-uniform flux profile).

The temperature gradient generates differential dilations of the structures; analogously, the gradient of irradiation dose – combined to the temperature gradient – determines differential growths of the structures due to void swelling.

These non-uniformities apply even among the faces of each assembly: as a consequence, differential (thermal or swelling) deformations are observed also at the level of single assembly.

Overall, the deformations can be considered as the sum of a uniform and a differential contribution. The uniform contribution determines an homothetic increase of the assembly sizes while preserving the shape; the differential contribution instead acts exactly the other way round: it changes the shape with no net increase of the size. This can be visualized in the two frames of Figure 1.

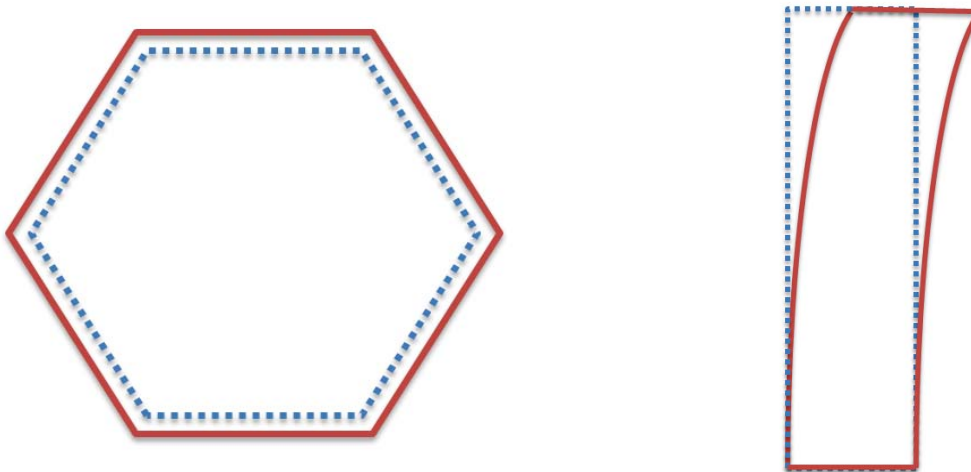


Figure 1. Effects of uniform (left) and differential (right) deformations.

This study will concentrate on the effect of differential deformations to retrieve the shape of an assembly at the end of its residence period in core.

### 3. Model description

The reference model for this study is the ALFRED [1] fuel assembly, as the assembly anticipated to be subject to the largest differential deformations. As shown in Figure 2, to the sake of this study the FA is made of 5 main sections:

- “**spike**”: is the foot of the FA, coupling the lower core plate for the correct positioning of the element;
- “**bottom shroud**”: is the lower section of the FA, where an hexagonal wrapper – enclosing the bundle of fuel pins – represents the structural part;
- “**funnel**”: is the central section of the FA, made of a reduced cross-section part so as to define the upper plenum for directing the coolant flow towards the steam generators;
- “**upper shroud**”: is the upper section of the FA, ; is made (as the bottom shroud) of an hexagonal wrapper, although the upper shroud only contains a ballast block in its upper part;
- “**upper head**”: it the FA head, meant for coupling with the upper core plate where spring cups are inserted to allow for free axial expansion of the FA.

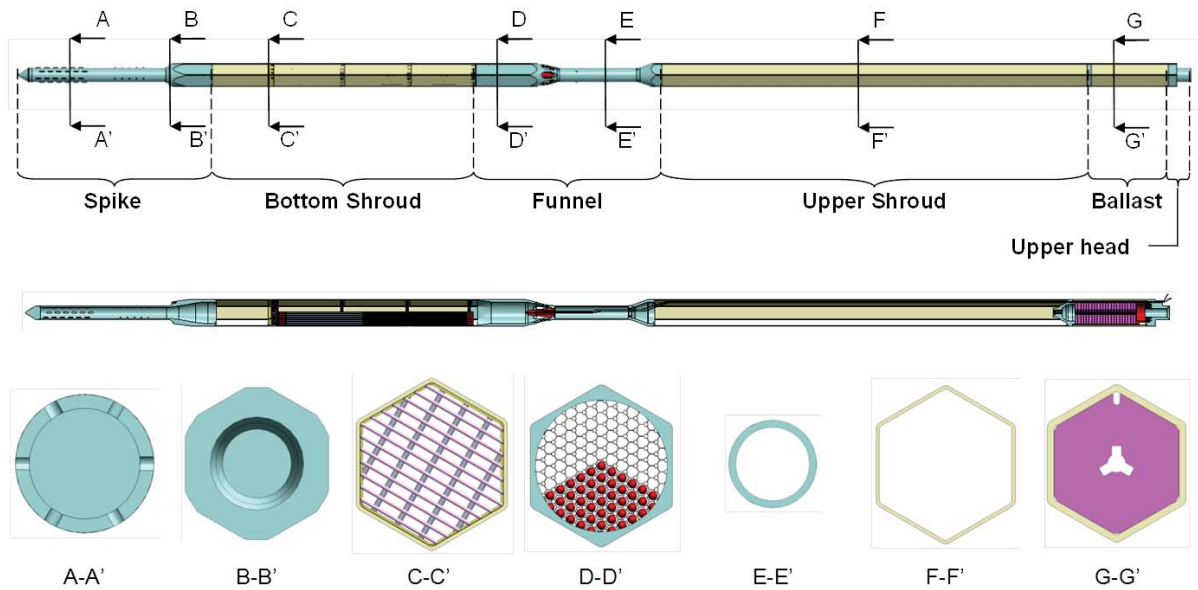


**Figure 2. View of the ALFRED FA [1].**

The analysis of the problem will concentrate on the study of the free deformation of a single FA. The focus will therefore be set on the hexagonal wrapper, as the main structure of an assembly, and limited to the portion which experiences temperature differences along its cross-section (as the source of thermal deformations) and/or significant differential fluence (i.e., above the threshold for which swelling is observed). The investigated section involves therefore an 81 cm long portion of the hexagonal wrapper in the bottom shroud.

In this section, the wrapper tube (Figure 3) has an inner flat-to-flat dimension of 159 mm, with walls 3.5 mm thick. Each FA is also positioned with 5 mm clearance on each side from the neighboring FAs. All dimensions refer to as-fabricated conditions, i.e.: before positioning in the reactor core, hence not including the core expansion at full power.

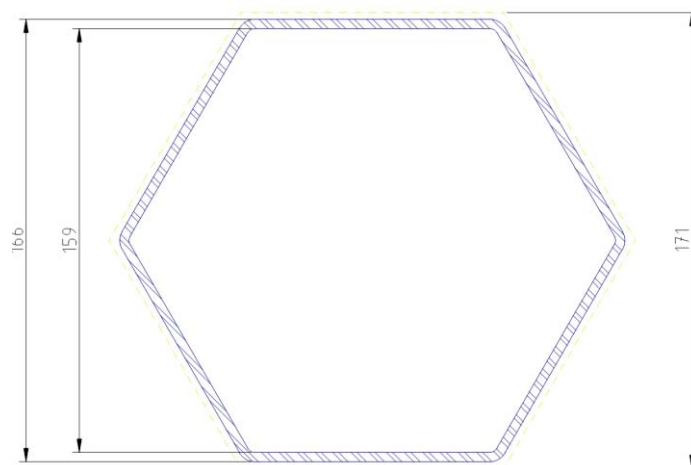


**Figure 3. Cross-section of the ALFRED wrapper (dimensions in [mm]).**

At given quotes of the wrapper, wearing pads are realized – on every face – by drawing. The pads therefore are protruded out of the outer faces, locally reducing the gap in such a way that, as soon as the core outlet temperature exceeds the nominal value set for full-power, the assemblies enter in contact with each other at the level of the pads.

This reduced gap is the actual clearance against which the results of this study will have to be compared.

#### 4. Methodology and assumptions

Propaedeutic to the study, the reference system is fixed at first, with the origin positioned, and the main axes oriented, as shown in Figure 4.

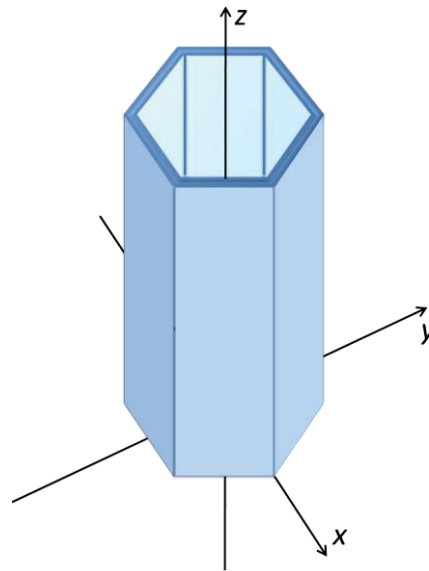


Figure 4. Model of analysis: definition of the reference system.

From the model described above, it is possible to calculate the deformations of each face at each axial quote, due to both thermal and swelling dilations. The differential equation describing the investigated deflection is therefore:

$$\frac{d^2y}{dz^2} = \frac{M_{tot}(z)}{E I} \quad , \quad (1)$$

where

$M_{tot}$  is the total bending moment due to differential temperature and swelling gradients;

$I$  is the moment of inertia of the wrapper;

$E$  is the Young modulus of the wrapper material.

By using the principle of superposition of the effects, eq. (1) becomes

$$\frac{d^2y}{dz^2} = \frac{M_{th}(z)+M_{sw}(z)}{E I} \quad , \quad (2)$$

where  $M_{th}$  and  $M_{sw}$  are the bending moments due to the thermal and swelling gradients, respectively.

The thermal bending moment can be made explicit as

$$M_{th}(z) = \int_A E \alpha(T) T(x, y) y dA \quad , \quad (3a)$$

where  $\alpha(T)$  is the linear expansion coefficient of the wrapper material.

Analogously, the swelling bending moment can be cast as

$$M_{sw}(z) = \int_A E \varepsilon_{sw}(x, y) y dA \quad , \quad (3b)$$

where  $\varepsilon_{sw}(x, y)$  is the swelling-induced deformation.

To solve the second order differential equation (2) boundary conditions are required. In this study, the fuel assembly is assumed as a beam fixed at the basis: this is consistent with the predicted assembly-diagrid coupling. The boundary conditions are therefore assumed as

$$\begin{aligned} y(0) &= 0 \\ \frac{dy}{dz}(0) &= 0 \quad , \end{aligned} \quad (4)$$

which translate the assumptions of no displacement and no rotation at the basis.

In order to solve numerically the problem, the fuel assembly is discretized in finite segments along the  $z$  axis, as shown in Figure 5, for each of which the solution will be retrieved so as to compose the overall solution incrementally.

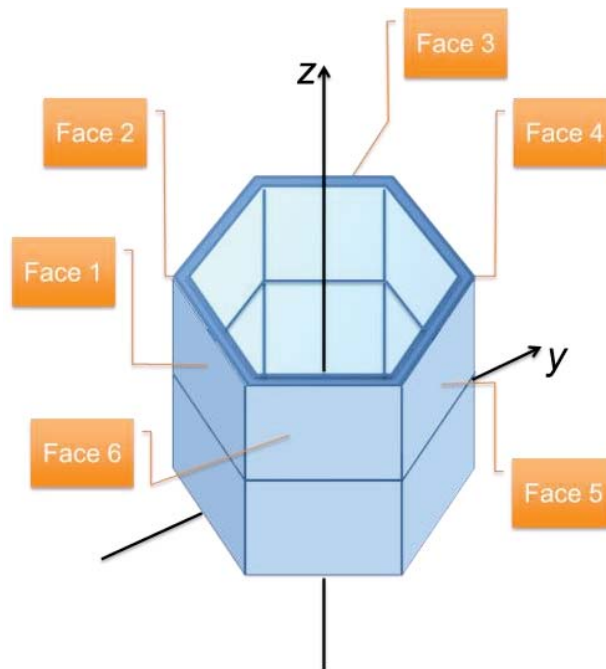


Figure 5. Model of analysis: axial segmentation of the wrapper and numbering of faces.

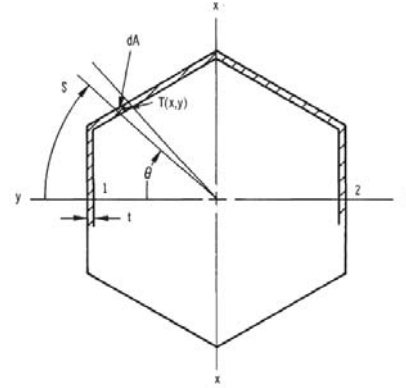
The solution of eqs. (3a) and (3b) at every axial elevation provides the bending moments as source in eq. (2). As simplifying hypotheses, it is assumed that:

- the temperature and flux distributions are uniform on each face of the wrapper;
- there is a perfect symmetry about the  $y$  axis (i.e., referring to Figure 5, faces 2 and 3 are at the same temperature and subject to the same flux of faces 6 and 5, respectively).

Under these hypotheses, the study can be limited to the plane containing the axes  $y$  and  $z$  only.

For the numerical solutions are defined (with reference to figure aside):

- $t$  the wrapper thickness;
- $b$  the length of a wrapper face;
- $d$  the flat-to-flat of the wrapper.



Accordingly, eqs. (3a) and (3b) become

$$M_{th}(z) = E_1 \alpha_1 (T_1) T_1 t d \frac{b}{2} - E_2 \alpha_2 (T_2) T_2 \frac{t}{\cos(30^\circ)} \frac{d^2}{4} + E_3 \alpha_3 (T_3) T_3 \frac{t}{\cos(30^\circ)} \frac{d^2}{4} - E_4 \alpha_4 (T_4) T_4 t d \frac{b}{2} \quad (3a')$$

$$M_{sw}(z) = E_1 \varepsilon_{sw1} t d \frac{b}{2} - E_2 \varepsilon_{sw2} \frac{t}{\cos(30^\circ)} \frac{d^2}{4} + E_3 \varepsilon_{sw3} \frac{t}{\cos(30^\circ)} \frac{d^2}{4} - E_4 \varepsilon_{sw4} t d \frac{b}{2} \quad (3b')$$

At each discrete quote  $i$ , the total bending moment will be the sum of the two contributions as resulting from eqs. (3a') and (3b'):

$$M_{tot i} = M_{th i} + M_{sw i} \quad (5)$$

varying, due to the different temperatures, fluxes (hence fluences), Young moduli and thermal expansion coefficients.

After computation of the total bending moment at each discrete quote, the deformation of the wrapper along the  $y$  axis can be obtained by integrating twice eq. (2); what is obtained is the displacement of each axial segment of the wrapper:

$$y_i = \frac{M_{tot i-1} z_i^2}{2 E_i I} + \frac{(M_{tot i} - M_{tot i-1}) z_i^3}{6 E_i I \Delta l} \quad (6)$$

where  $\Delta l$  is the length of each axial segment of the wrapper, here assumed constant. Analogously, the rotation of each segment can be expressed as

$$\frac{dy_i}{dz} = \theta_i = \frac{(M_{tot i} + M_{tot i-1}) \Delta l}{2 E_i I} \quad (7)$$

The two equations (6) and (7) allow to retrieve the overall displacement of each wrapper segment incrementally as

$$y_i = \sum_{k=1}^i y_k + \sum_{k=1}^{i-1} \Delta l \sum_{j=1}^k \theta_j \quad (8)$$

The graphical representation of the obtained solution is shown in Figure 6.

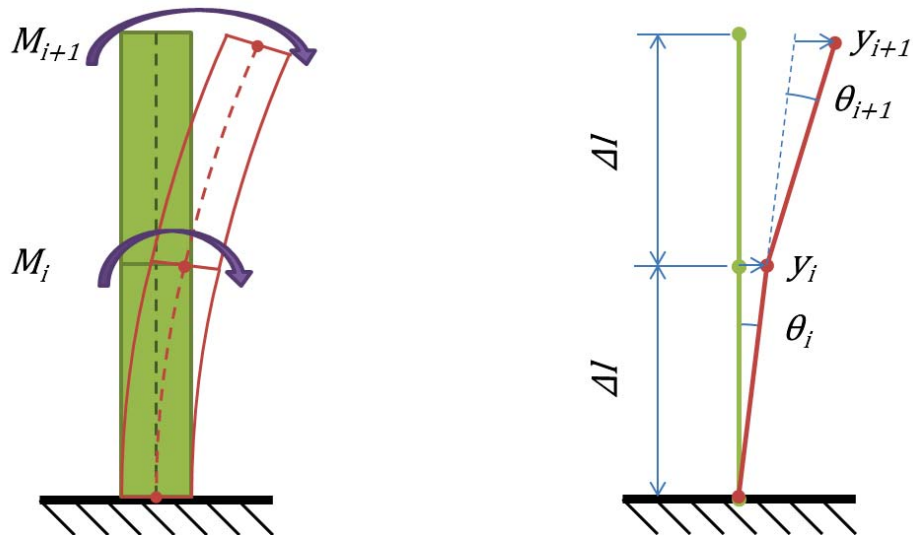


Figure 6. Representation of the bending moments acting on each wrapper segment (left) and of the deformations and rotations as resulting from the solution of the problem (right).

## 5. Results

### 5.1. Single fuel assembly

The described methodology is applied at first to the FA where the peak power and a significant flux gradient are experienced; the FA where these conditions occur is shown in Figure 7. It is worth noting that, in this specific case, the approximation set forth before, that the temperature and fluence gradients vary only along one direction in the plane – the  $y$  axis (here oriented radially) – holds true due to the position in the general core symmetry.

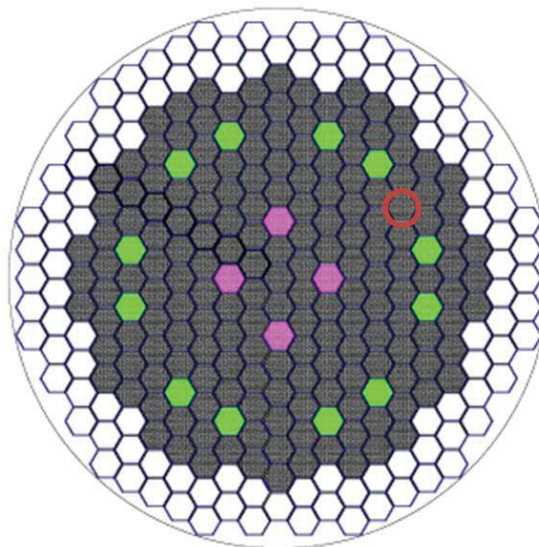


Figure 7. ALFRED core map, with position of the peak FA marked by a red circle.

The calculated profile of the deformed FA is shown in Figure 8, exhibiting a maximum displacement of 0.364 mm atop the assembly.

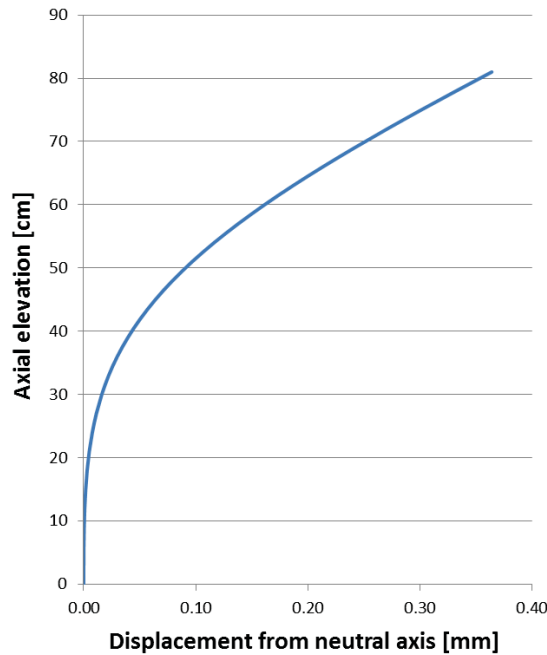


Figure 8. Deformed profile of the peak FA.

This is due to the fact that, even though no internal moment acts to enhance the deformation of the FA outside of the analyzed region, the angle of rotation at the final section projects the rest of the FA along the tangent, magnifying the displacement from the original axis.

### 5.2. Row of adjacent fuel assemblies

A very interesting analysis results from considering the deformations of a series of FAs in a row, and notably the radial row containing the peak FA. The same methodology is applied again to each element, and the results shown in Figure 9.

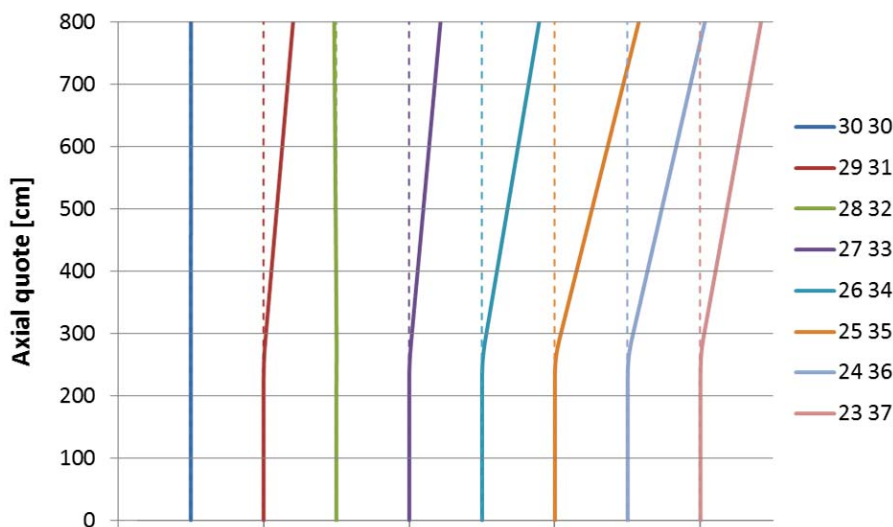


Figure 9. Reference (dotted lines) and deformed (solid lines) profiles of FAs in a radial row.

 <b>Ricerca Sistema Elettrico</b>	Sigla di identificazione	Rev.	Distrib.	Pag.	di
	ADPFISS – LP2 – 156	0	L	11	11

## 6. Conclusions

The present work was aimed at setting the bases for the design of the core restraint system for ALFRED, being the latter one of the most important components of the whole core system because of its manifold functions, many of which safety-related.

The study here presented was aimed at providing an initial estimate for the free deformations of the FAs at the end of irradiation. This estimate indeed can be used to size the interaction forces that will be developed among the FAs, and in turn to identify the most appropriate design of the core restraint system to fulfill all the identified requirements.

The final results are shown in Figure 9, where the deformed profiles of all the FAs belonging to a radial row are plotted against the reference, non-deformed profiles, and respecting the mutual (as fabricated, i.e., 5 mm) distances to permit appreciating the extent each FA is deformed.

As can be seen, despite the low-swelling material used for the wrapper, due to the peculiar length of the FAs the deformations at the assembly heads are such to completely close the inter-assembly clearance. Even more, these deformations will determine remarkable forces at the level of spacing pads, where the clearance is much reduced to realize an anti-compaction means to the core.

Despite the simplicity of the model, and the assumptions adopted for the present study, this result already permits retrieving a remarkable consideration: due to the originality of the design of the assemblies – provided with a very long stem so as to emerge from the melt – very little information will be borrowable from the core restraint systems designed and implemented in the past, requiring a special effort to conceive a solution specifically tailored for ALFRED.

## References

- [1] G. Grasso *et al.* The core design of ALFRED, a demonstrator for the European lead-cooled reactors. *Nucl. Eng. Des.* **278**:287-301 (2014).
- [2] D.A. Kucera and D. Mohr. BOW-V: a CDC-3600 program to calculate the equilibrium configurations of a thermally bowed reactor core. Technical Report ANL/EBR-014, ANL, January 1970.